THE ASTROPHYSICAL JOURNAL, 508:899–907, 1998 December 1

OBSERVATIONS OF CORRELATED WHITE-LIGHT AND EXTREME-ULTRAVIOLET JETS FROM POLAR CORONAL HOLES

Y.-M. WANG, N. R. SHEELEY, JR., D. G. SOCKER, R. A. HOWARD, G. E. BRUECKNER, D. J. MICHELS, D. MOSES, AND O. C. ST. CYR[1]
E. O. Hulburt Center for Space Research, Naval Research Laboratory, Washington, DC 20375-5352
A. LLEBARIA
Laboratoire d'Astrophysique Spatiale, F-13376 Marseille Cedex 12, France
AND
J.-P. DELABOUDINIÈRE
Institut d'Astrophysique Spatiale, F-91405 Orsay Cedex, France
Received 1998 June 5; accepted 1998 July 8

ABSTRACT

Time-lapse sequences of white-light images recorded with the Large Angle Spectrometric Coronagraph (LASCO) on the *Solar and Heliospheric Observatory* (*SOHO*) frequently show long, narrow structures moving outward over the Sun's polar regions at high apparent speeds. By comparing the LASCO observations with Fe XII λ195 spectroheliograms made with the Extreme-ultraviolet Imaging Telescope (EIT) on *SOHO* between 1997 April and 1998 February, we have identified 27 correlated white-light and extreme-ultraviolet (EUV) jet events. In each case, the EUV jet was observed near the limb of the polar coronal hole 20–60 minutes before the corresponding white-light jet was registered in the coronagraph's 2–6 $R_\odot$ field of view. The jets originate near flaring EUV bright points and are presumably triggered by field line reconnection between magnetic bipoles and neighboring unipolar flux. The leading edges of the white-light jets propagate outward at speeds of 400–1100 km s^{-1}, whereas the bulk of their material travels at much lower velocities averaging around 250 km s^{-1} at heliocentric distances of 2.9–3.7 $R_\odot$. These lower velocities may reflect the actual outflow speeds of the background polar wind.

Subject headings: interplanetary medium — solar wind — Sun: corona — Sun: magnetic fields

1. INTRODUCTION

With its unprecedented sensitivity and its temporal and spatial resolving power, the Large Angle Spectrometric Coronagraph (LASCO) on the *Solar and Heliospheric Observatory* (*SOHO*) has revealed a number of unexpected dynamical features of the white-light corona. These discoveries include the small density enhancements ("blobs") that continually drift outward through the streamer belt (see Sheeley et al. 1997; Wang et al. 1998) and the narrow, jetlike structures that are seen fleetingly above the polar regions (see St. Cyr et al. 1997). The blobs form near the cusps of helmet streamers and appear to be carried outward by an ambient slow solar wind. Here we are concerned with the polar jets, whose properties are in some ways complementary to those of the streamer blobs.

The detection of faint, jetlike features moving radially outward over the poles with apparent speeds of up to 1000 km s^{-1} raises obvious questions about their relation to the fast solar wind. Are we seeing the polar wind or tracers thereof? Are we observing the switching-on or switching-off of polar plumes? Alternatively, are the "jets" an artifact of the image-subtraction procedure, resulting (for example) from the rotation or sideways displacement of plumes or streamers?

These questions can be addressed most simply by locating the source of the jets on the Sun. High–time-resolution observations of the polar coronal holes with the Extreme-ultraviolet Imaging Telescope (EIT) on *SOHO* indeed show short-lived jets (Gurman et al. 1996; Moses et al. 1997), which in turn are reminiscent of those discovered earlier in soft X-rays with *Yohkoh* (Shibata et al. 1992). It is natural to ask whether the white-light structures observed with LASCO are just the extensions of the extreme-ultraviolet (EUV) jets into the outer corona, despite the much smaller spatial dimensions of the latter (see St. Cyr et al. 1997). To resolve this question, we have searched the LASCO/EIT database for positional and temporal correlations between the two kinds of events.

2. OBSERVATIONS

The LASCO instrument (Brueckner et al. 1995) comprises three coronagraphs with overlapping fields of view: C1 (1.1 $R_\odot \lesssim r \lesssim 3\ R_\odot$), C2 (2 $R_\odot \lesssim r \lesssim 6\ R_\odot$), and C3 (4 $R_\odot \lesssim r \lesssim 32\ R_\odot$). (In this paper, r denotes apparent heliocentric distance as seen projected onto the plane of the sky.) Both C2 and C3 are externally occulted white-light coronagraphs, whereas the internally occulted C1 coronagraph is equipped with a Fabry-Perot interferometer that can be tuned to a number of important spectral lines, including Fe XIV λ5303 and Fe X λ6374. Each coronagraph has its own 1024 × 1024 pixel CCD camera, which records images with a 2 pixel resolution of 11″ (C1), 24″ (C2), and 112″ (C3).

Most of the LASCO jets are detected with the C2 coronagraph. Because they are relatively faint and traverse the C2 field of view in $\lesssim$2 hours, the jets are best seen in time-lapse movies constructed from images taken 20–60 minutes apart. During 1996–1998, such C2 movies typically showed 3–4 jets per day over the polar regions, although the occurrence rate was highly variable and the actual number may depend on the sensitivity of the instrument and on the observational cadence. Relatively few jets are observed with C3, both because of its lower spatial resolution and because the jets fade rapidly with distance from the Sun. Only one

[1] Computational Physics, Inc., Fairfax, VA.

jet was unambiguously seen with the narrowband C1 instrument.

The EIT telescope (Delaboudinière et al. 1995) employs normal-incidence, multilayer mirrors to provide full-disk images of the Sun out to $r \sim 1.4\ R_\odot$ in any one of four emission lines: Fe IX λ171, Fe XII λ195, Fe XV λ284, and He II λ304. The images are again recorded on a 1024 × 1024 pixel CCD with a two-pixel resolution of 5″. The jets appear inside the polar coronal holes in Fe XII λ195, whose emission peaks at a temperature of 1.6×10^6 K. Because of their high speeds and short lifetimes, the jets are best observed in sequences of Fe XII images taken only a few minutes apart. Jetlike features may also be present in Fe IX λ171 and Fe XV λ284, but their identification is hampered by the relative scarcity of high-cadence EIT observations in these lines.

From 1997 April to 1998 March, the EIT instrument routinely obtained a full-disk Fe XII λ195 spectroheliogram every 10–20 minutes; meanwhile, LASCO images were generally taken every 20–60 minutes. Because the data coverage during this time was superior to that earlier in the *SOHO* mission, we have restricted our systematic search for correlated EIT/LASCO jets to this more recent period. By first identifying relatively bright jets in C2 running-difference movies and then examining the underlying region in Fe XII λ195 spectroheliograms taken 20–60 minutes earlier, we found 27 cases in which a white-light jet appeared to have an EUV counterpart inside the polar coronal hole.

Table 1 gives the dates, times of occurrence, and position angles of the correlated EIT/LASCO jets. The two times listed for each jet refer to the main EUV event and to the first appearance of the white-light jet in a C2 image. Correspondingly, position angles (measured eastward from the north pole) are specified both at the solar surface and at the inner edge of the C2 field of view. It may be noted that the difference between the two position angles increases systematically with angular distance from the pole, as expected if the jet trajectories are aligned with the Sun's diverging, nonradial polar magnetic field lines.

TABLE 1

CORRELATED EIT/LASCO JETS

Date	EUV Event (UT)	Position Angle ($r \simeq 1\ R_\odot$) (deg)	Enters C2 (UT)	Position Angle ($r \gtrsim 2\ R_\odot$) (deg)
1997 Apr 2	14:10	347	14:57	335
1997 Apr 2	22:49	192	23:24	202
1997 Apr 3	13:03	343	13:40	326
1997 Apr 5	10:48	349	11:26	338
1997 Apr 11	09:06	4	10:05	9
1997 Apr 19	05:24	182	06:30	183
1997 May 15....	15:50	180	16:30	181
1997 Jun 19	08:51	172	09:31	166
1997 Jun 19	10:33	171	11:31	164
1997 Jun 19	10:47	170	11:31	161
1997 Jul 15.....	09:20	343	10:16	320
1997 Aug 5	11:53	350	12:20	343
1997 Aug 5	21:30	350	22:17	345
1997 Sep 28	11:29	14	12:05	22
1997 Oct 21.....	05:47	356	06:30	352
1997 Oct 30.....	12:19	179	12:52	177
1997 Nov 16	15:22	350	15:55	342
1997 Nov 24	03:09	171	03:45	164
1997 Dec 5.....	03:03	357	03:55	359
1997 Dec 16	02:51	181	03:09	180
1997 Dec 27	20:59	347	21:16	334
1998 Jan 14	17:53	171	18:28	163
1998 Jan 15	15:22	176	15:55	172
1998 Jan 15	18:24	176	19:24	172
1998 Jan 26	07:46	1	08:41	0
1998 Jan 26	09:57	1	10:36	358
1998 Feb 7.....	01:35	342	02:27	318

Some examples of the correlated EIT/LASCO events are displayed in Figure 1. In each case, the Fe XII jet originates from the vicinity of a bright point (or small magnetic bipole) near the limb of the polar coronal hole. Inspection of the images in the left and middle columns of Figure 1 suggests that the EUV jet is somewhat displaced from the bright point, as is especially evident in the 1997 May 15, 1997 September 28, and 1998 January 14 events. The corresponding white-light jets appear in the C2 field of view beyond 2 $R_\odot$ (Fig. 1, *right-hand column*) after a time lapse that depends on the observational cadence but is typically about 30–40 minutes. The long, slightly bent structure seen on May 15 actually consists of two white-light jets, the earlier, outermost one presumably originating from the same flaring bright point as the later one. In the C2 difference image of November 24, the jet is just entering the field of view with its leading edge at $r \sim 2.7\ R_\odot$; since the EIT image shows the Fe XII counterpart leaving the solar surface 36 minutes earlier, we can immediately estimate a propagation speed of ~ 550 km s^{-1} for the front end of this jet.

Figure 2 focuses on the eruption of a jet at the south pole on 1997 October 30. In the sequence of Fe XII λ195 images in the left-hand column, we first see a diffuse feature that represents an EUV polar plume rooted just inside the limb. A bright point then erupts just to the east of the plume, accompanied (at 12:19 UT) by an outward ejection with a jetlike spike. The whole base area remains bright until at least 12:32 UT; by 12:49 UT, however, the region (including the earlier plume) has largely faded away. The sequence of images in the right-hand column shows the leading edge of the white-light jet crossing the 2–6 $R_\odot$ C2 field of view between 12:52 and 14:26 UT. From the time lapse between the EUV eruption at 12:19 UT and the first observation of the white-light jet at 12:52 UT, we may estimate a speed of order 600 km s^{-1} for the leading edge of the jet.

Figure 3 shows a particularly energetic EIT/LASCO event that occurred on 1997 August 5. Although a faint "precursor" may be seen at 11:36 UT, the main EUV jet erupts around 11:53 UT, following which a long, bright spike appears in the white-light image at 12:20 UT. The eruption occurs alongside a wide EUV polar plume with a bright base region (see *bottom left-hand panel* of Fig. 3). By 13:02 UT, the white-light jet extends across the entire C2 field of view, although its brightness decreases rapidly with heliocentric distance. The searchlight structure then progressively fades away, becoming barely detectable by 15:35 UT. The bottom right-hand panel of Figure 3 shows the jet in polarized white light at 12:45 UT, when its intensity at $r \sim 2.55\ R_\odot$ exceeds that of the background K corona by over 40% (Fig. 4).

The August 5 example illustrates the typical geometry of a white-light jet. It has an angular width (measured about its own axis) of 3°–4°, somewhat less than that characteristic of a polar plume (Saito 1965; Newkirk & Harvey 1968). As for a polar plume (see, e.g., Campbell, Moore, & Baker 1923), the axis of the jet does not lie along a line intersecting the center of the Sun. This deviation from a purely radial geometry, which increases with colatitude (polar angle) at a

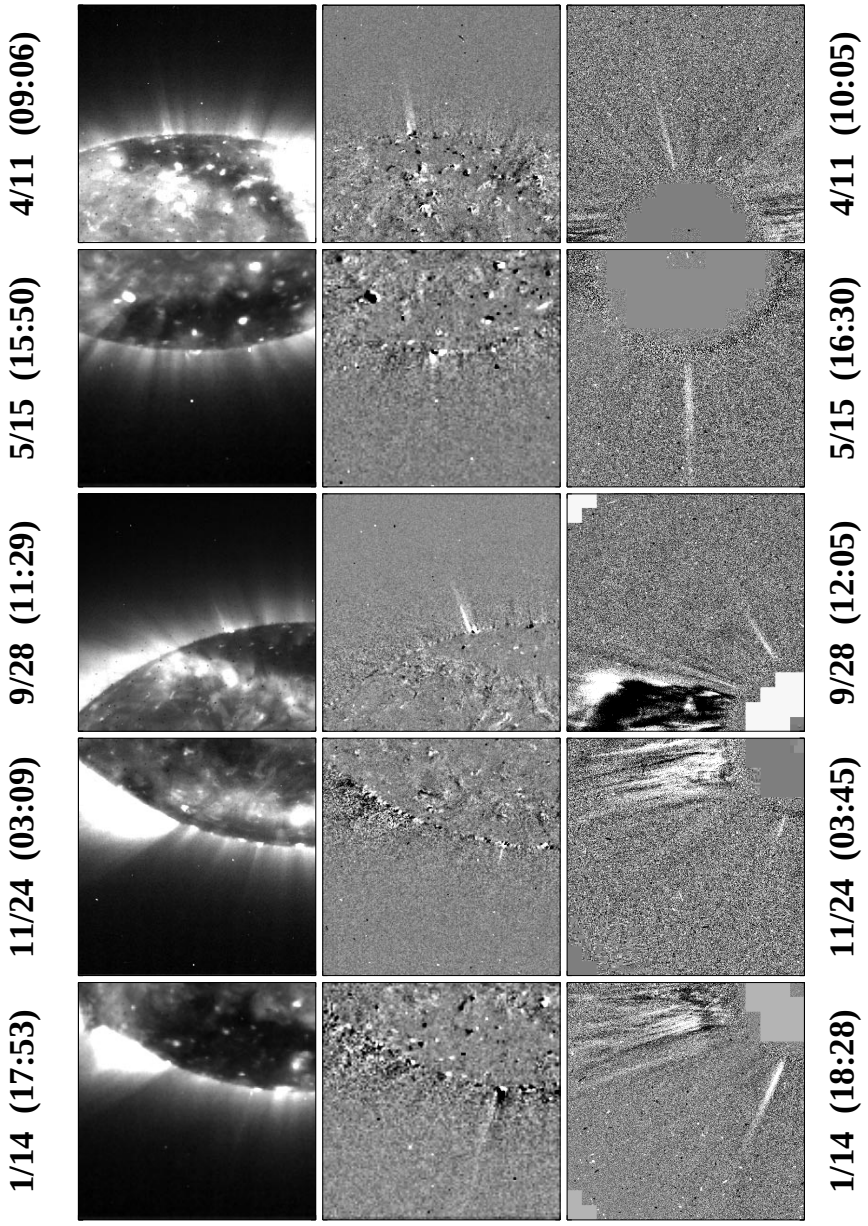

FIG. 1.—Five examples of correlated EIT/LASCO polar jets: 1997 April 11 (*top row*), 1997 May 15 (*second row*), 1997 September 28 (*third row*), 1997 November 24 (*fourth row*), 1998 January 14 (*bottom row*). EUV event in Fe XII λ195 (*left-hand panels*); time of observation (UT) is given at the left. In every case, the jet originates near a bright point located close to the limb of the polar coronal hole. EUV intensities relative to an EIT image taken 10–20 minutes before the event (*middle panels*). White-light intensities relative to a C2 image taken just before the jet appears in the coronagraph's 2–6 $R_\odot$ field of view (*right-hand panels*); time of observation is at the right.

given r, is a consequence of the strong poleward concentration of the Sun's large-scale magnetic field near sunspot minimum and the tendency for the flux distribution to become increasingly uniform with heliocentric distance: the polar field lines must therefore bend progressively equatorward in the corona (see Wang & Sheeley 1992).

Figure 5 shows a bright jet on 1997 June 19, which was observed not only in white light and in Fe XII λ195, but also in the coronal green (Fe XIV λ5303) and red (Fe X λ6374) lines with the C1 coronagraph. The double-barreled structure of the white-light jet appears to correspond to the pair of spikes visible in the EUV spectroheliogram at 10:47 UT. The eruption originates from a closely spaced pair of bright points at the limb of the south polar coronal hole. The detection of the jet in Fe X, Fe XII, and Fe XIV implies electron temperatures that span the whole range (1–2) $\times 10^6$ K.

On 1998 January 26, a spectacular EUV event occurred at the north pole, to be observed subsequently in white light with both the C2 and C3 coronagraphs. As indicated by Figure 6, the eruption occurred as a looplike appendage formed at the eastern flank of a bright point, which itself underwent a marked decrease in intensity just before the eruption. At the start of the event near 09:57 UT we see a bright Fe XII structure with a strong helical twist rising above the newly formed loop. At 10:05 UT, a second jet erupts from the west side of the bright point and then fades away by 10:21 UT. The original jet, which now forms a long, straight structure, undergoes a very gradual decay, remaining visible beyond 10:40 UT. The C2 image shows

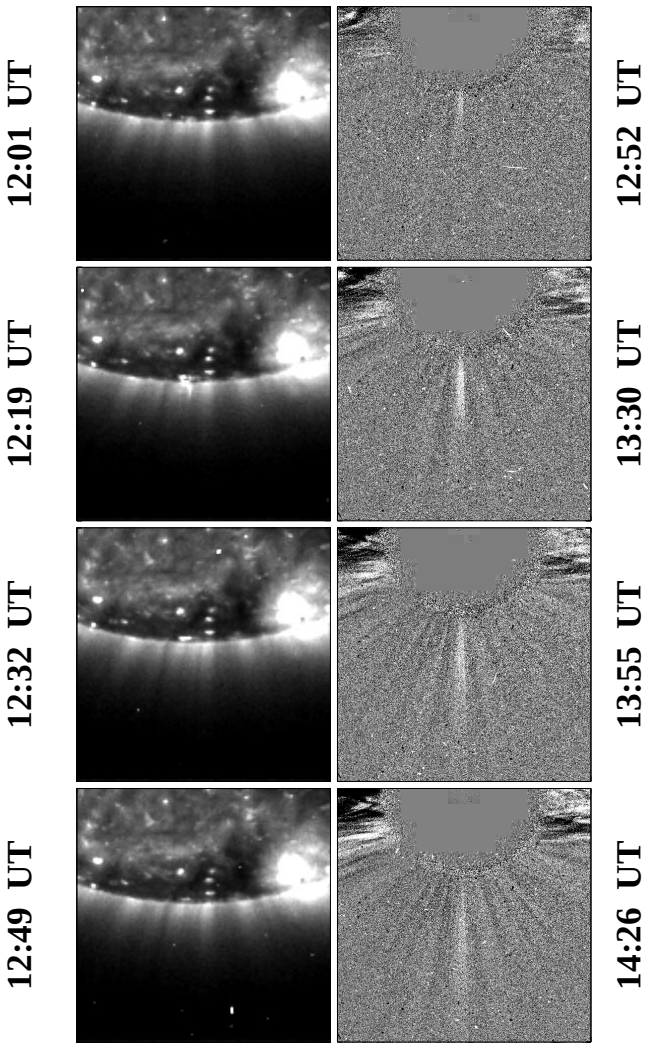

FIG. 2.—Correlated EIT/LASCO jet event, 1997 October 30. Time sequence of Fe XII λ195 images showing the eruption of a jet inside the south polar coronal hole at 12:19 UT (*left-hand panels, top to bottom*). Time-lapse sequence of C2 images relative to a base image taken at 12:27 UT, showing a white-light jet traversing the coronagraph's 2–6 $R_\odot$ field of view (*right-hand panels, top to bottom*).

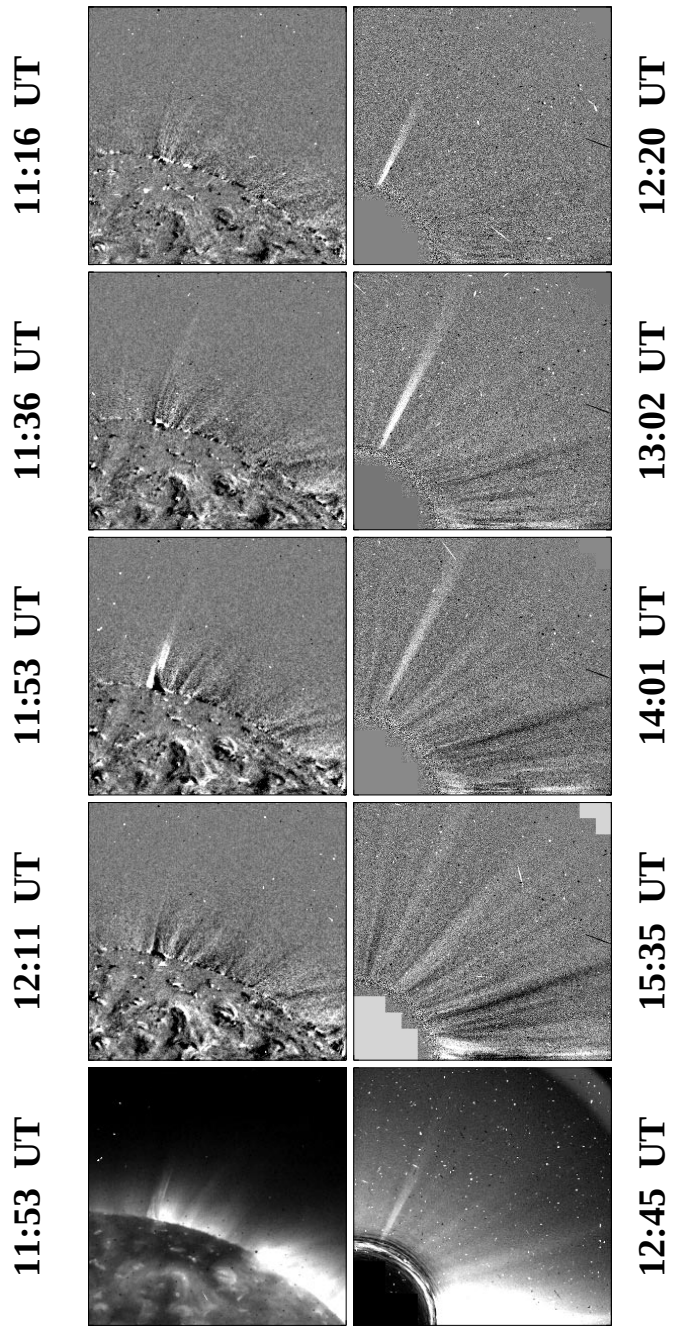

FIG. 3.—Energetic jet event on 1997 August 5. Time-lapse sequence of Fe XII λ195 images relative to a base image taken at 10:45 UT, showing the eruption of a large EUV jet inside the north polar coronal hole at 11:53 UT (*left-hand column, top four panels*). Time-lapse sequence of C2 images relative to a base image taken at 11:59 UT, showing a bright white-light jet traversing the coronagraph's 2–6 $R_\odot$ field of view (*right-hand column, top four panels*). Undifferenced Fe XII λ195 image of the main EUV event at 11:53 UT (*bottom left-hand panel*). Undifferenced C2 polarized image of the white-light jet at 12:45 UT (*bottom right-hand panel*).

the white-light counterpart extending to $\sim 3\ R_\odot$ 40 minutes after the EUV eruption, implying a leading-edge velocity of roughly 600 km s^{-1}.

It is very common to observe a succession of white-light jets at approximately the same position angle over periods ranging from hours to days. The jet displayed in Figure 3 was only one of six that originated from the same region of the north polar hole between 07:57 UT on August 5 and 02:18 UT on August 6. The June 19 (Fig. 5) and January 26 (Fig. 6) events were each preceded by an earlier eruption from the same region, which likewise produced correlated EIT/LASCO jets. Figure 7 shows an especially striking example of repetitive jet activity from 1996 May 31 to June 2, when seven white-light jets occurred in succession above the same ephemeral region near the south polar limb.

3. JET SPEEDS

The dynamical properties of the jets can be investigated by means of height-time measurements. For each jet, we have derived a number of different velocities, which depend on where along the jet and when during its evolution the measurements are made:

1. *The leading-edge velocity*, $v_{\rm lead}$.—Here the "leading edge" is defined as the outermost part of the jet that can be visually distinguished as an enhancement above the background in running-difference images. The velocity estimate is based on a linear least-squares fit to the successive leading-edge positions, which generally include one EIT

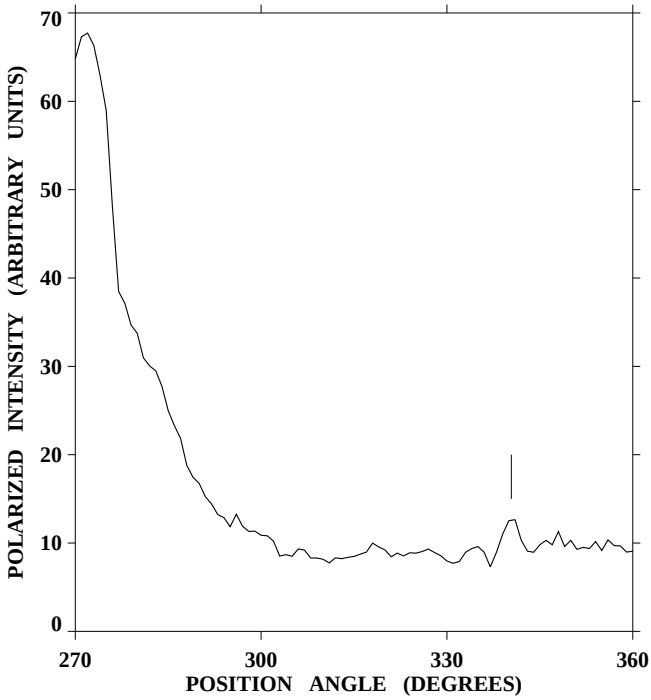

FIG. 4.—Plot of polarized intensity (pB) vs. position angle ϕ at $r = 2.55$ $R_\odot$, 12:45 UT on 1997 August 5. The jet is located near $\phi = 340°$; the much larger peak at $\phi \sim 270°$ represents the west equatorial streamer (see *bottom right-hand panel* of Fig. 3). The jet gradually becomes submerged in the background corona at greater distances.

point near the solar surface and from one to three LASCO C2 measurements beyond 2 $R_\odot$.

2. *The centroidal velocity of the white-light jet*, $v_{\rm cen}$.—To locate the "centroid" of the jet on a given C2 image, we first determine the relative intensity distribution along the jet, defined as

$$I_{\rm rel}(s) \equiv \left(\frac{r}{R_\odot}\right)^2 \frac{[I(s) - I_{\rm base}(s)]}{I_{\rm base}(s)} . \quad (1)$$

Here s represents the coordinate position along the axis of the jet, r is the apparent heliocentric distance, I refers to the local value of the total intensity in the current C2 image, and $I_{\rm base}$ to the corresponding value in a fixed base frame taken just before the jet appears in the C2 field of view. In this definition of $I_{\rm rel}$, the two intensities are subtracted to isolate the contribution of the jet; normalizing by the base-image intensity cancels out the effect of a radially dependent vignetting function (see Brueckner et al. 1995), while multiplying by r^2 offsets the falloff of intensity along the jet due to its quasi-radial expansion. The position of the centroid, $r_{\rm cen}$, is found by fitting the sum of a Gaussian and a second-order polynomial to the peak of $I_{\rm rel}(s)$ (see Fig. 8, which illustrates the time evolution of the relative intensity distribution for a C2 jet observed on 1997 August 5). Finally, $v_{\rm cen}$ is derived by fitting a straight line to 2–5 successive measurements of $r_{\rm cen}$, where 2.5 $R_\odot \lesssim r_{\rm cen} \lesssim 5.0$ $R_\odot$. Measurements outside this radial range are difficult to carry out because of the large stray-light contribution to $I_{\rm base}$ near 2 $R_\odot$ and the fading of the jet relative to the background toward 6 $R_\odot$.

3. *The initial velocity of the centroid*, $v_{\rm init}$.—Here the EUV event and the first C2 observation of the jet are used to estimate the speed at which the centroid propagates from the solar surface to the inner portion of the C2 field of view. (The cadence of the EIT observations was not sufficiently high to allow velocities to be determined for the EUV jets themselves.)

Table 2 gives the values of $v_{\rm lead}$, $v_{\rm cen}$, and $v_{\rm init}$ derived for the 27 jets listed in Table 1. The leading-edge velocities range from 400 to 1100 km s^{-1}, with a median value of 593 km s^{-1}; the uncertainty in the individual measurements is estimated to be of order $\pm 25\%$. The centroidal velocities of the C2 jets are much lower, varying between 140 and 360 km s^{-1} and averaging around 250 km s^{-1}. As noted above, the centroid measurements were made at heliocentric distances between 2.5 and 5.0 $R_\odot$ (mean distance $r \sim 3.3$ $R_\odot$). Finally, Table 2 shows that $v_{\rm init}$ is usually substantially larger than $v_{\rm cen}$ (but smaller than $v_{\rm lead}$), implying that the bulk of the jet material decelerates as it propagates from the solar surface into the C2 field of view.

In Figure 9, the centroidal velocities $v_{\rm cen}$ are plotted against the mean radius at which each velocity measurement was made. The plot emphasizes the relatively small spread of $v_{\rm cen}$ about its mean value of 249 km s^{-1}. It also suggests a tendency for $v_{\rm cen}$ to increase with heliocentric distance; when the measured points are fit with a straight line (correlation coefficient 0.48), the rate of increase in the region 2.9–3.7 $R_\odot$ is found to be $dv_{\rm cen}/dr \sim 118$ km s^{-1} $R_\odot^{-1}$.

Figure 10 shows a scatter diagram of $v_{\rm lead}$ versus $v_{\rm cen}$. The evident lack of a correlation between the two velocities suggests that the bulk of the jet material has already been decelerated to the outflow rate of the background medium by the time it enters the C2 field of view (assuming that such a background medium exists).

The large difference between $v_{\rm lead}$ and $v_{\rm cen}$ implies that the jets elongate rapidly as they propagate through the corona.

TABLE 2

JET SPEEDS

Date	Time of Measurements (UT)	$v_{\rm lead}$ (km s^{-1})	$v_{\rm cen}$ (km s^{-1})	$v_{\rm init}$ (km s^{-1})
1997 Apr 2	13:57–16:12	413	260	426
1997 Apr 2	22:40–00:15	856	279	721
1997 Apr 3	13:03–14:56	815	137	568
1997 Apr 5	10:39–12:19	486	322	330
1997 Apr 11	09:06–10:27	537	246	369
1997 Apr 19	05:24–07:35	496	295	292
1997 May 15.....	15:50–16:30	811	161	600
1997 Jun 19	08:34–09:31	689	...	627
1997 Jun 19	10:33–12:27	694	308	360
1997 Jun 19	10:47–12:27	703	209	430
1997 Jul 15.....	09:20–11:07	537	217	362
1997 Aug 5.....	11:36–14:01	1091	268	697
1997 Aug 5.....	21:09–23:37	691	252	450
1997 Sep 28	11:29–13:28	709	185	502
1997 Oct 21	05:34–07:23	560	299	478
1997 Oct 30	12:19–13:55	473	171	548
1997 Nov 16	15:22–16:55	486	359	555
1997 Nov 24	03:09–04:15	593	259	502
1997 Dec 5	03:03–05:08	624	324	369
1997 Dec 16	02:34–03:58	522	263	525
1997 Dec 27	20:49–22:36	601	183	583
1998 Jan 14	17:36–19:24	798	284	435
1998 Jan 15	15:22–16:55	699	255	600
1998 Jan 15	18:24–20:58	542	183	340
1998 Jan 26	07:46–09:38	425	287	322
1998 Jan 26	09:57–10:36	576	...	416
1998 Feb 7	01:35–03:55	490	224	348

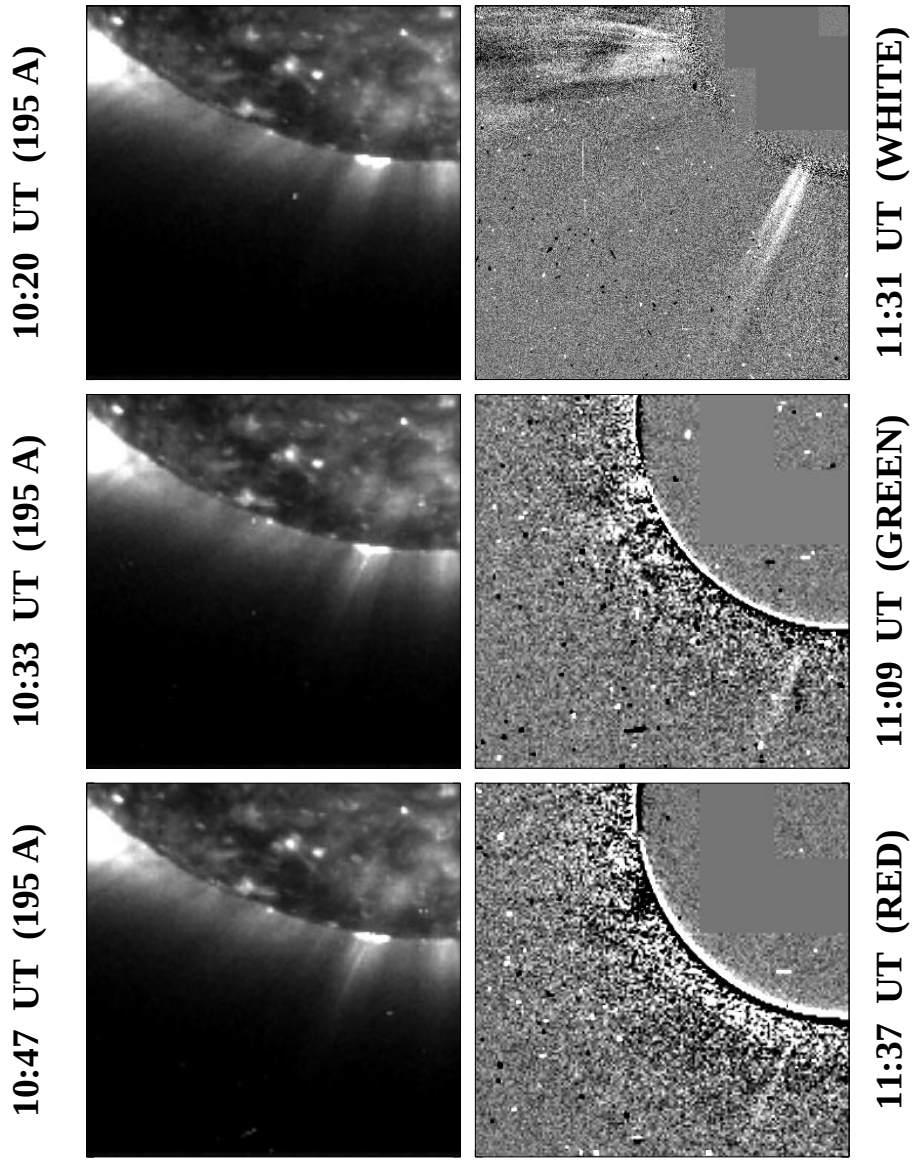

FIG. 5.—"Twin jet," 1997 June 19. Sequence of Fe XII λ195 images showing jets emitted from a closely spaced pair of bright points inside the south polar coronal hole (*left column*); two simultaneous jets may be seen at 10:47 UT. Note the presence of diffuse plume "haze" above the bright points. Double jet observed in white light with the C2 coronagraph (*top right-hand panel*; difference between images taken at 11:31 UT and 10:29 UT). Fe XIV λ5303 (green line) difference image recorded with the C1 coronagraph, showing a single jet structure extending outward from 1.1 $R_\odot$ at 11:09 UT (*middle right-hand panel*). Base image is at 10:43 UT. Fe X λ6374 (red line) difference image recorded with the C1 coronagraph, showing a single, narrow jet structure extending outward from 1.1 $R_\odot$ at 11:37 UT (*bottom right-hand panel*). Base image is at 10:37 UT.

Based on the median values $v_{\rm lead} \sim 593$ km s^{-1} and $v_{\rm cen} \sim 259$ km s^{-1}, the distance between the leading edge and the centroid of the jet increases at a rate of $\sim 1.7\ R_\odot$ hour^{-1}. The progressive lengthening and attenuation of the white-light jets may be seen directly from time-lapse sequences of C2 images, such as those displayed in Figures 2 and 3.

4. DISCUSSION

4.1. *Origin of Jets*

All of the correlated EUV/white-light jets that we have identified originate near one or more bright points. The eruption is generally accompanied by a change in the intensity and shape of the underlying structure. As is evident from the EUV images of May 15, September 28, and January 14 displayed in Figure 1, the jet is actually somewhat displaced from the bright point, which in the May 15 example clearly has the form of a small loop. In the simplest physical interpretation, the EUV events are triggered by magnetic reconnection between newly emerged bipoles and nearby unipolar flux, as has been suggested for X-ray jets (Shibata et al. 1992; Shimojo, Shibata, & Harvey 1998). According to this scenario, the majority-polarity end of the bipole opens up and becomes the site of the jet, while its minority-polarity end reconnects with the neighboring monopole to form a new closed loop.

Many (but by no means all) of the events originate near EUV polar plumes; examples include the jets of April 11 (Fig. 1), August 5 (Fig. 3), and June 19 (Fig. 5). The proximity can be explained by the fact that bright points are often found near the bases of EUV plumes. In Wang (1998), it was suggested that both plumes and jets are energized by reconnection between bipoles and unipolar flux concentrations within the polar holes, but that the reconnection is driven

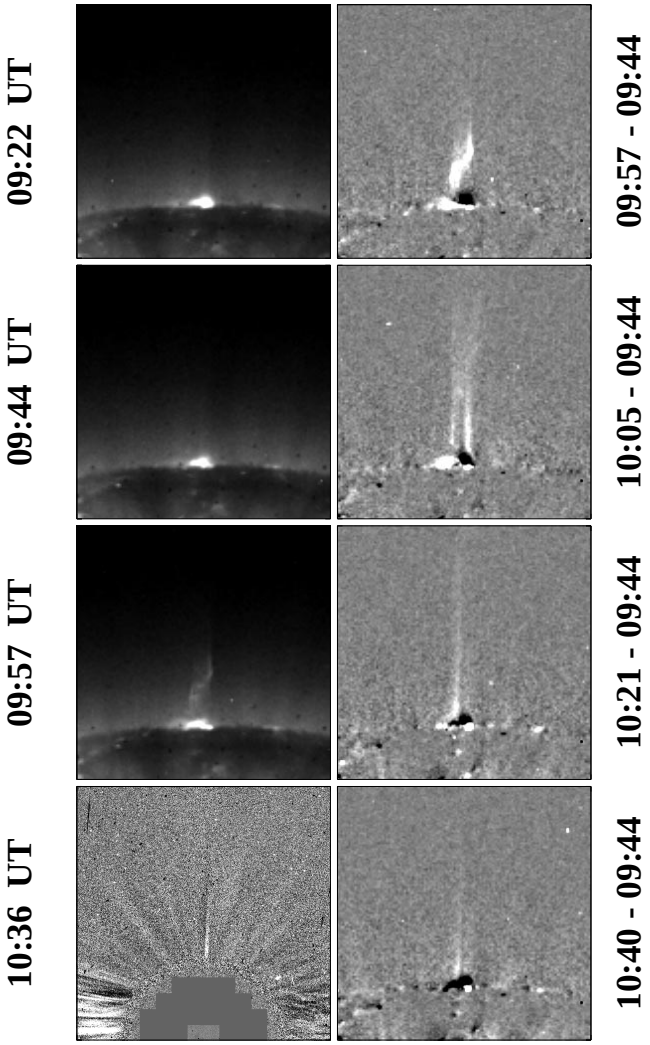

FIG. 6.—"Corkscrew" jet event at the north pole, 1998 January 26. Sequence of (undifferenced) Fe XII λ195 images showing bright point before and at the moment of eruption (*left column, top three panels*). Time-lapse sequence of Fe XII λ195 images showing the ejection of material after the eruption (*right-hand column*). Base image is at 09:44 UT. White-light jet observed with the C2 coronagraph (*bottom left-hand panel*; difference of images taken at 10:36 UT and 09:38 UT).

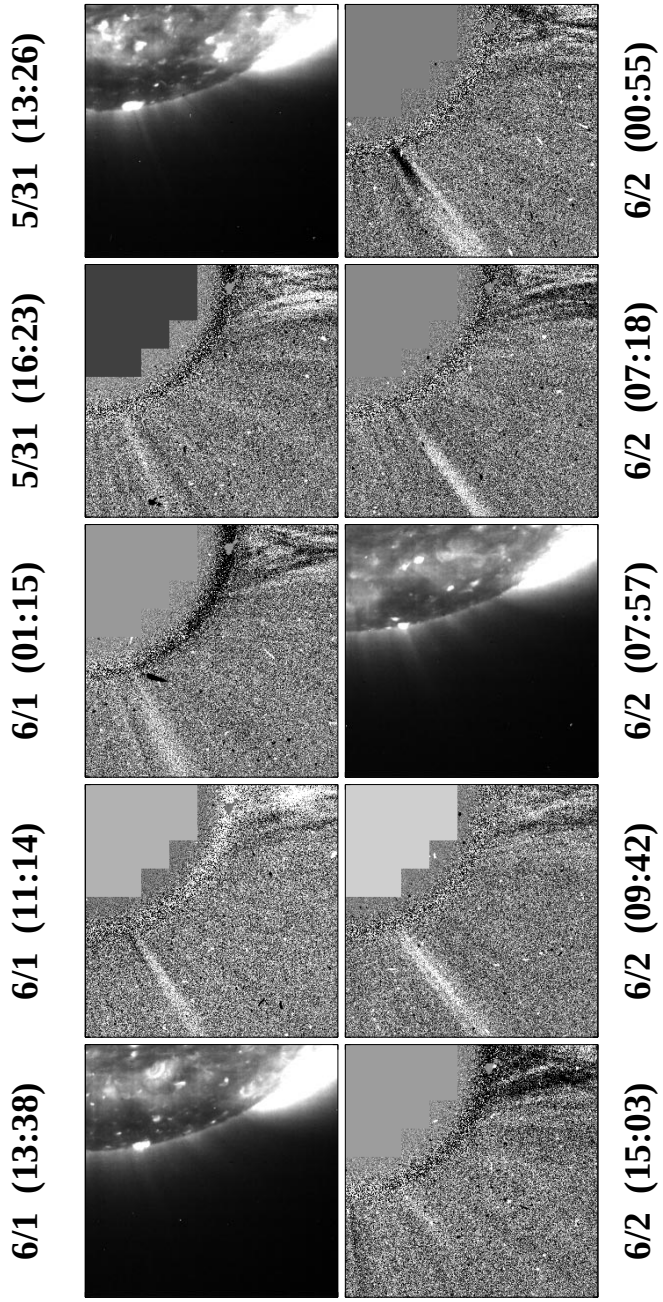

FIG. 7.—Succession of seven white-light jets observed above a long-lived, compact Fe XII λ195 feature, 1996 May 31–June 2. The jets are shown here in C2 difference images.

by the supergranular flow field in the case of the plumes and by flux emergence in the case of the jets. Since the timescale for the supergranular flow is much longer than that for flux emergence, the plumes are long lived and quiescent whereas the jets are short lived and flarelike.

Remarkably, all of the EIT/LASCO jets listed in Table 1 originated very close to (within 30″ of) the polar limb. The visibility of these jets is enhanced in white light because they lie near the sky plane and in the EUV because they protrude well above the limb and are subject to limb brightening. The actual distribution of jet events within the polar coronal holes is expected to be far more uniform than our observationally biased sample suggests.

High-cadence running-difference movies made from Fe XII λ195 images give the impression that numerous faint jets are continually being emitted from bright points within the polar holes. A similar impression of many white-light jets near the noise level is obtained from LASCO C2 movies. We are unable to determine how much these low-level jet events contribute to the emission of polar plumes or to the mass flux from the polar coronal holes.

4.2. *Propagation of Jets*

In § 1 we remarked on the apparent disparity in spatial scales between the small EUV jets and their white-light counterparts, which are often seen extending across the entire C2 field of view. The discrepancy can now be understood in terms of the existence of a large velocity differential along the length of the jet, whose leading edge travels at 2–3 times the speed of its central portion. Some EUV jets may also be active over relatively long periods: Figure 6 shows a case in which material continues to be ejected from the source up to 1 hour after the main EUV event.

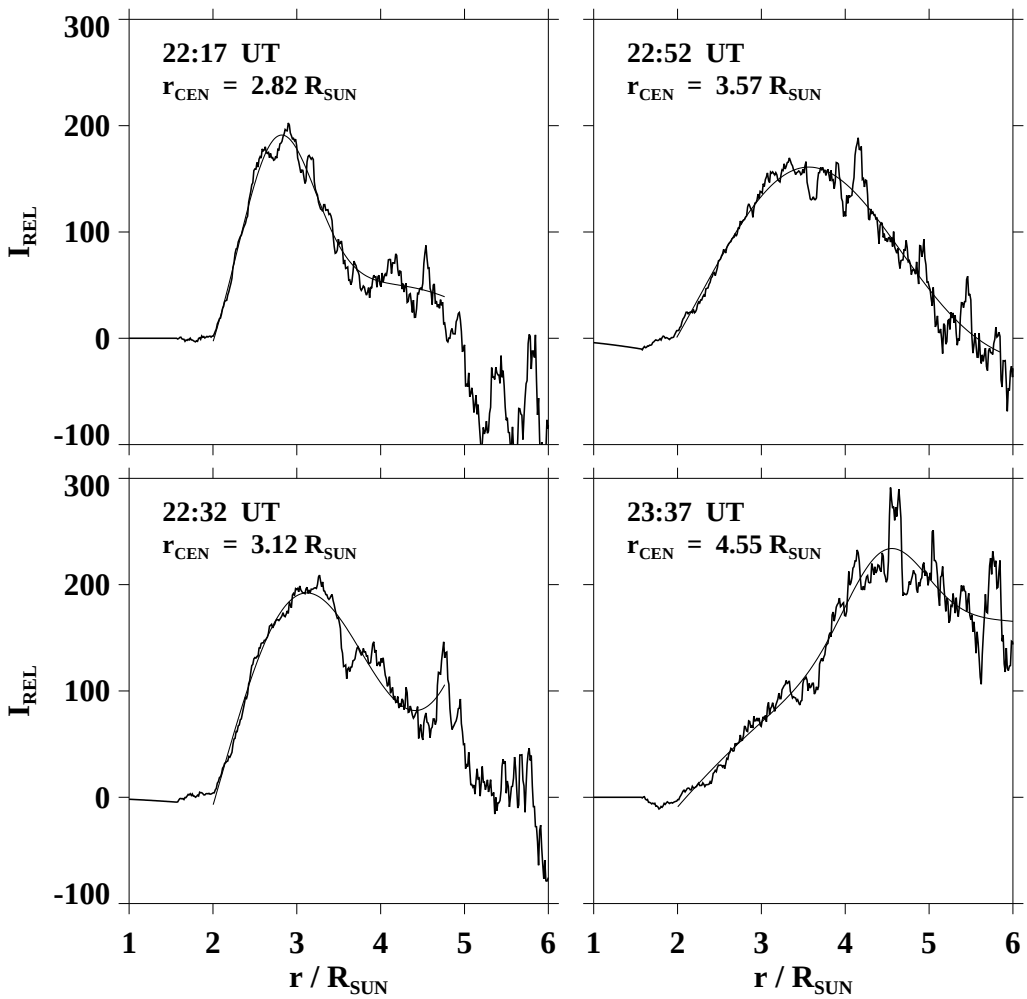

FIG. 8.—Relative intensity distribution $I_{rel}(s) \equiv (r/R_\odot)^2[I(s) - I_{base}(s)]/I_{base}(s)$ along the axis of a white-light jet observed on 1997 August 5, shown at 22:17 UT, 22:32 UT, 22:52 UT, and 23:37 UT. (Base image is at 21:16 UT.) The centroid of the jet at each successive time, r_{cen}, is determined by fitting the sum of a Gaussian and a quadratic to the peak of $I_{rel}(r)$, as indicated by the smooth curve in each panel.

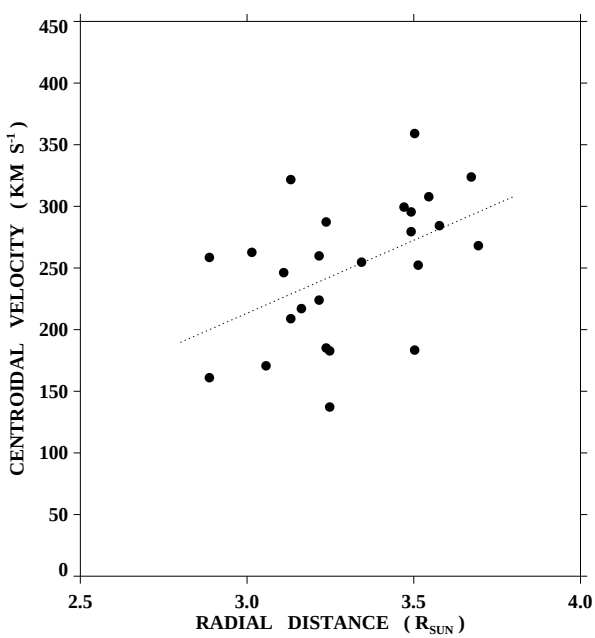

FIG. 9.—Centroidal velocities of 25 white-light jets plotted against the mean radius at which the measurements were made. The dotted line represents a linear least-squares fit to the data points, given by $v_{cen} = -142 + 118(r/R_\odot)$ km s^{-1}.

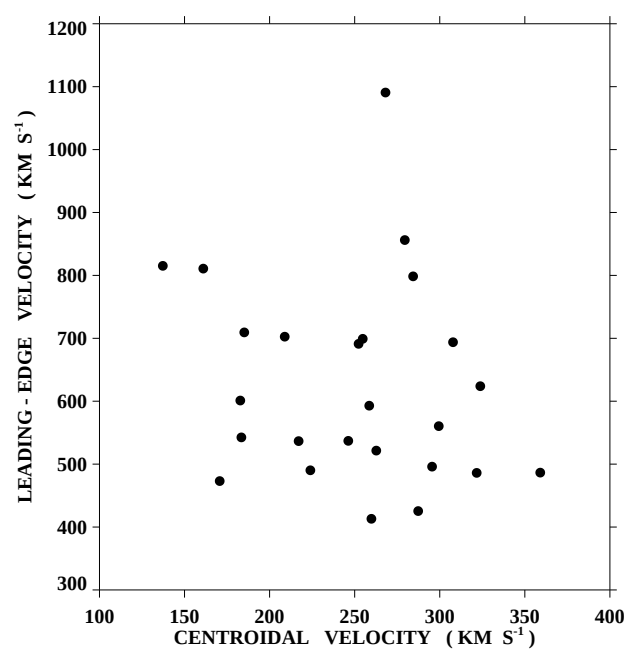

FIG. 10.—Scatter diagram of v_{lead} vs. v_{cen}, demonstrating the absence of correlation between the two velocities.

By comparing v_{cen} with v_{init} (Table 2), we inferred that the main portion of the jet undergoes substantial deceleration as it propagates from the lower corona into the C2 field of view beyond 2 $R_\odot$. The deceleration is most simply attributed to the effect of gravity on matter ejected impulsively near the solar surface, where the escape speed is $v_{esc} \simeq 618$ km s^{-1}. Thus, if no further acceleration were to take place after the ejection, the initial velocity would have to be greater than 437 km s^{-1} for the jet material to travel beyond $r = 2$ $R_\odot$. The values of v_{init} shown in Table 2 suggest that the bulk of the material is ejected at speeds below v_{esc} and is consequently strongly decelerated. In contrast, the leading edges of the jets leave the Sun with speeds in excess of v_{esc} and thus experience relatively little deceleration.

Since we have no evidence for downflows in either the EIT or the C2 images, we infer that in situ acceleration prevents the bulk of the jet material from falling back onto the Sun after it is ejected. This inference is supported by the measured values of v_{cen}, which fall in a relatively narrow range between $\sim$140 and $\sim$360 km s^{-1} (see Fig. 9), and by the lack of any correlation between v_{cen} and v_{lead} (see Fig. 10), which suggests that the centroidal velocities are essentially independent of the impulsive events that triggered the jets. If the latter interpretation is correct, then v_{cen} may simply represent the speed of the background polar wind or that in a polar plume. Indeed, the behavior of $v_{cen}(r)$ suggested by Figure 9 appears consistent with polar wind models in which the sonic point occurs at $r \sim 2.5$ $R_\odot$ (see Table 1 and Fig. 2 in Wang 1994).

5. CONCLUSIONS

Our main results may be summarized as follows:

1. Based on 27 correlated events identified between 1997 April and 1998 February, we conclude that the white-light polar jets observed beyond 2 $R_\odot$ with LASCO are the outer coronal extensions of the EUV jets recorded by EIT.

2. All of the EIT/LASCO jets originated near EUV bright points inside the polar coronal holes. At least one-half of the events occurred in the vicinity of EUV polar plumes. As in the case of soft X-ray jets, the EUV events are most likely triggered by reconnection between small magnetic bipoles and nearby unipolar flux concentrations.

3. All of the white-light jets in our study originated very near the polar limb and were thus located close to the plane of the sky. If allowance is made for such visibility effects, the actual frequency of the jets probably far exceeds the rate of 3–4 per day that were typically seen in C2 running-difference movies. An important question that remains to be addressed is whether large numbers of faint jets at or below the detection threshold of the EIT and LASCO instruments are present, and, if so, whether they contribute significantly to the mass flux from the polar coronal holes.

4. A succession of jets are often ejected from the same region. As observed in white light, the repetitive jet activity may last from hours to days.

5. White-light jets have characteristic angular widths (measured about their nonradial axes) of $\sim$2°–4°. Like the large-scale polar magnetic field, the deviation of their axes from the radial direction increases with polar angle.

6. The leading edges of the white-light jets propagate outward at speeds ranging from 400 to 1100 km s^{-1} (median $\sim$590 km s^{-1}), whereas their centroidal velocities are much lower, ranging from 140 to 360 km s^{-1} (median $\sim$260 km s^{-1}) in the region 2.9–3.7 $R_\odot$. The large velocity differential causes the jets to elongate with time.

7. The bulk of the jet material is ejected with less than the surface escape velocity and decelerates between 1 and 2 $R_\odot$.

8. The relatively narrow range of centroidal velocities ($v_{cen} \simeq 250 \pm 110$ km s^{-1}) measured around 3.3 $R_\odot$ and the absence of any correlation between v_{cen} and v_{lead} suggest that the bulk of the jet material moves through the C2 field of view at the speed of the background polar wind.

The last conclusion is potentially the most important of this study, since it raises the possibility that the jets can be used to determine the dynamical properties of the polar wind itself in the immediate vicinity of the Sun. Indeed, Figure 9 suggests the presence of a sonic point near $r \sim 2.5$ $R_\odot$. Such velocity measurements need to be extended in the future to include a much larger sample of white-light jets.

This study was made possible only through the efforts of the entire LASCO/EIT team. We are especially grateful to S. E. Paswaters, N. B. Rich, and D. Wang for assistance with the data processing. Financial support was provided by NASA and by the Office of Naval Research.

REFERENCES

Brueckner, G. E., et al. 1995, Sol. Phys., 162, 357
Campbell, W. W., Moore, J. H., & Baker, R. H. 1923, PASP, 35, 163
Delaboudinière, J.-P., et al. 1995, Sol. Phys., 162, 291
Gurman, J. B., et al. 1996, Eos, 77, 559
Moses, D., et al. 1997, Sol. Phys., 175, 571
Newkirk, G., Jr., & Harvey, J. 1968, Sol. Phys., 3, 321
St. Cyr, O. C., et al. 1997, in Proc. 31st ESLAB Symp. (ESA SP-415) (Noordwijk: ESA), 103
Saito, K. 1965, PASJ, 17, 1
Sheeley, N. R., Jr., et al. 1997, ApJ, 484, 472
Shibata, K., et al. 1992, PASJ, 44, L173
Shimojo, M., Shibata, K., & Harvey, K. L. 1998, Sol. Phys., 178, 379
Wang, Y.-M. 1994, ApJ, 435, L153
———. 1998, ApJ, 501, L145
Wang, Y.-M., & Sheeley, N. R., Jr. 1992, ApJ, 392, 310
Wang, Y.-M., et al. 1998, ApJ, 498, L165